Self-Assembled Three-Dimensional Hierarchical Umbilicate Bi 2 WO 6 Microspheres from Nanoplates: Controlled Synthesis, Photocatalytic Activities, and Wettability

ARTICLE *in* THE JOURNAL OF PHYSICAL CHEMISTRY C · MARCH 2009

Impact Factor: 4.77 · DOI: 10.1021/jp810726d

6 AUTHORS, INCLUDING:

ma Dekun
Wenzhou University
62 PUBLICATIONS **1,144** CITATIONS
SEE PROFILE

Shaoming Huang
Wenzhou University
118 PUBLICATIONS **4,582** CITATIONS
SEE PROFILE

THE JOURNAL OF PHYSICAL CHEMISTRY C

Article

Self-Assembled Three-Dimensional Hierarchical Umbilicate BiWO Microspheres from Nanoplates: Controlled Synthesis, Photocatalytic Activities, and Wettability

Dekun Ma, Shaoming Huang, Wenxiu Chen, Shengwei Hu, Fangfang Shi, and Kelei Fan

J. Phys. Chem. C, **2009**, 113 (11), 4369-4374• DOI: 10.1021/jp810726d • Publication Date (Web): 24 February 2009

Self-Assembled Three-Dimensional Hierarchical Umbilicate Bi_2WO_6 Microspheres from Nanoplates: Controlled Synthesis, Photocatalytic Activities, and Wettability

Dekun Ma,* Shaoming Huang,* Wenxiu Chen, Shengwei Hu, Fangfang Shi, and Kelei Fan

Nanomaterials and Chemistry Key Laboratory, Wenzhou University, Wenzhou, Zhejiang 325027, P. R. China

Received: December 5, 2008; Revised Manuscript Received: January 17, 2009

Self-assembled three-dimensional (3D) hierarchical umbilicate Bi_2WO_6 microspheres from nanoplates have been synthesized by a new controllable hydrothermal route on a large scale. It was found that citrate played multifold roles in the formation process of Bi_2WO_6 hierarchical microspheres in our reaction system. In order to obtain well-assembled Bi_2WO_6 microspheres, $NaHCO_3$ was used to adjust pH values of the reaction solution and establish a buffer system by the equilibrium of the formation and dissociation of carbonic acid. On the basis of XRD analysis and TEM observation of the products at the different reaction time periods, the formation mechanism of Bi_2WO_6 hierarchical microspheres was proposed. UV−vis diffuse reflectance spectra indicated that as-synthesized Bi_2WO_6 hierarchical microspheres had absorption in both UV and visible light areas. The BET surface area of the sample was ca. 24.1 m^2/g, which was 35 times higher than that of the Bi_2WO_6 powder prepared by the solid-state reaction method. The hierarchical umbilicate Bi_2WO_6 microspheres exhibited good photocatalytic activity in degradation of Rhodamine-B (RhB) under 150 W Xe lamp light irradiation. In addition, the wettability of Bi_2WO_6 films fabricated by as-obtained Bi_2WO_6 microspheres was also studied.

1. Introduction

During the past decades, controlled synthesis of the primary building blocks such as nanoparticles, nanowires, nanobelts, and nanoplates has made great progress.[1−4] Many recent efforts have been focused on the hierarchical assembly of these simple nanostructures into ordered superstructures or complex architectures, which is a crucial step toward the realization of functional nanosystems and offers opportunities to study their novel collective optical, electronic, and magnetic properties.[5−8] Generally, hierarchical architectures can be formed through several methodologies such as biomimetic mineralization,[9] polymer directed self-assembly,[10] oriented aggregation of nanoscale building units,[11] Kirkendall-type diffusion,[12] hard- and soft-templating synthesis,[13−15] and sequential nucleation and growth.[16] Among various methods, the chemical-solution-phase self-assembly method is simple, effective, and inexpensive for large-scale production. On the basis of different driving mechanisms, such as van der Waals forces, $\pi-\pi$ interactions, electrostatic forces, hydrogen bonding, and hydrophobic interactions, a number of self-assembly processes have been achieved in the chemical solution phase. Most of the assembly process in the solution phase deals with surfactant or polymer that is often used to promote (or tune) the ordered alignment of primary nanobuilding blocks.[17] However, the use of a relatively high content of surfactants or polymers will make the assemblies easy to collapse when the surfactants or polymers are removed or dissolved in the solvent, which results in difficulties with their potential applications as nanodevices.[18] Therefore, it is still a challenge to explore effective routes for directing nanoscale units by the self-assembly mode into complex and stable architectures.

Bi_2WO_6 is one of the simplest members of the Aurivillius oxide family of layered perovskites with the general formula $Bi_2A_{n-1}BnO_{3n+3}$ (A = Ca, Sr, Ba, Pb, Na, K; B = Ti, Nb, Ta, Mo, W, Fe; and n = number of perovskite-like layers $(A_{n-1}B_nO_{3n+1})^{2-}$), which are structurally composed of alternating perovskite-like and fluorite-like blocks.[19] It has many attractive and important physical properties such as ferroelectric piezoelectricity, pyroelectricity, catalytic behavior, oxide anion conducting, a nonlinear dielectric susceptibility, and luminescent properties.[20−26] Kudo and Hijii first reported that Bi_2WO_6 had photocatalytic activity for O_2 evolution, and Zou et al. revealed that Bi_2WO_6 could degrade the organic compound under visible light irradiation.[27,28] Their work showed that Bi_2WO_6 could perform as an excellent photocatalytic material or solar energy transfer material. However, all Bi_2WO_6 samples were prepared by solid-state reaction in their work, and the photocatalytic activity was not high. It is well-known that nanoscale photocatalysts usually have high photocatalytic activity because of their special morphologies, large specific surface areas, and high efficiency of electron−hole separation. Hence, many efforts have been made to synthesize nanosized Bi_2WO_6 to improve its photocatalytic activity.[29−32] Nevertheless, it is difficult to separate and recycle nanoscale photocatalysts at present. Comparatively speaking, 3D microscale architectures fabricated from nanosized building blocks hold many advantages, such as high photocatalytic activity, abundant transport paths for small organic molecules, and comparative ease of separation and recyclability. There have been several successful strategies to prepare 3D Bi_2WO_6 architectures such as a triblock Pluronic P123-assisted hydrothermal route,[33] PVP-assisted hydrothermal methods,[34,35] and the use of an excess amount of a tungstate precursor (10%) and an acidic condition during the hydrothermal process.[36]

In this work, we synthesized Bi_2WO_6 3D hierarchical umbilicate microspheres by a newly designed hydrothermal self-assembly process. Citrate anions were used as a complexing agent to control nucleation and growth of Bi_2WO_6 in a hydrothermal process. Additionally, it could selectively absorb at the crystal face of the Bi_2WO_6 nanoplates and direct the orientation and self-assembly of these primary nanobuilding blocks, resulting in the formation of Bi_2WO_6 hierarchical architectures. The photocatalytic properties of the as-obtained 3D hierarchical architectures were investigated under Xe lamp

* Authors to whom correspondence should be addressed. Email: dkma@wzu.edu.cn; smhuang@wzu.edu.cn. Fax: +86 577 88373064. Tel: +86 577 88373031.

10.1021/jp810726d CCC: $40.75
Published on Web 02/24/2009

light irradiation. Most of the hierarchical nanostructured binary metal oxide substrates can exhibit special wettability, which has aroused much interest because of their great advantages in applications.[37−39] However, there are only a few reports on the wettability of hierarchical nanostructured ternary metal oxide.[40] Hence, we prepared a Bi_2WO_6 film fabricated by as-synthesized Bi_2WO_6 hierarchical microspheres and studied its wettability.

2. Experimental Details

All chemical reagents in this work were purchased from the Shanghai Chemical Company. They were of analytical grade and used without further purification. Ultrapure water was used throughout the experimental process.

2.1. Synthesis of 3D Hierarchical Umbilicate Bi_2WO_6 Microsphere. In a typical procedure for the synthesis of 3D hierarchical umbilicate Bi_2WO_6 microspheres, 1 mmol of $Bi(NO_3)_3 \cdot 5H_2O$ was added into 40 mL aqueous solution containing 1 mmol of citric acid to form the metal−citrate complex. After vigorous stirring for 10 min, 0.5 mmol of $Na_2WO_4 \cdot 2H_2O$ and 2 mmol of $NaHCO_3$ were introduced into the above solution. After further agitation for 5 min, the solution was poured into a stainless steel autoclave with a Teflon liner of 60 mL capacity and heated at 200 °C for 18 h. After the autoclave had cooled to room temperature, the products were separated centrifugally and washed with ultrapure water and absolute ethanol three times. Then, the products were dried under vacuum at 60 °C for 4 h.

2.2. Fabrication of Bi_2WO_6 Films. Bi_2WO_6 films were obtained by drop-casting an ethanolic suspension of as-synthesized hierarchical umbilicate Bi_2WO_6 microspheres onto Si wafers.

2.3. Characterization. Powder X-ray diffraction (XRD) was carried out with a Bruker D8 Advance X-ray diffractometer using Cu Kα radiation ($\lambda = 0.154\,18$ nm) at a scanning rate of 8°/min in the 2θ range from 10° to 70°. Field emission scanning electron microscopy (FE-SEM) images and energy-dispersive X-ray (EDX) spectroscopy were taken on a Nova NanoSEM 200 scanning electron microscope. Transmission electron microscopy (TEM) observation and selected area electron diffraction (SAED) patterns were performed with a JEOL JEM 2010 high-resolution transmission electron microscope (HRTEM), using an accelerating voltage of 200 kV. IR spectra were obtained on a Bruker EQUINOX 55 Fourier transform IR (FTIR) spectrometer from 4000 to 500 cm^{-1}. The samples and KBr crystal were ground together and then the mixture was pressed into a flake for IR spectroscopy. The optical diffuse reflectance spectra were recorded on a UV2501PC (Shimadzu) using $BaSO_4$ as reference. The Brunauer−Emmett−Teller (BET) surface area was measured at JW-K nitrogen adsorption surface area pore size distribution analyzer (Beijing JWGB Sci. & Tech. Co., Ltd.) using adsorption data. Photocatalytic activity of hierarchical umbilicate Bi_2WO_6 microspheres was evaluated by degradation of RhB under Xe lamp light. In every experiment, 0.1 g of the photocatalyst was added to 100 mL of RhB solution (10^{-5} mol/L). Before illumination, the suspensions were magnetically stirred in the dark for 12 h to ensure the establishment of an adsorption−desorption equilibrium between the photocatalysts and RhB. After that, the solution was exposed to Xe lamp light irradiation under magnetic stirring. At given time intervals, 3 mL aliquots were sampled and centrifuged to remove the photocatalyst particles. Then, the filtrates were analyzed by recording variations of the absorption band maximum (553 nm) in the UV−vis spectra of RhB by using a Shimadzu UV2501PC spectrophotometer. The wettability of the as-prepared Bi_2WO_6 films was analyzed by measurement of the water contact angle (CA) using an Easydrop contact angle system (KRÜSS GmbH, Germany). All of the measurements were carried out at room temperature.

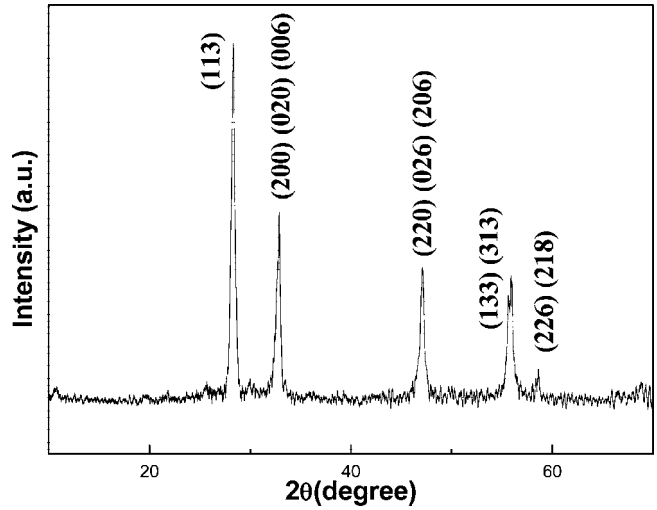

Figure 1. XRD pattern of the as-synthesized products at 200 °C for 18 h.

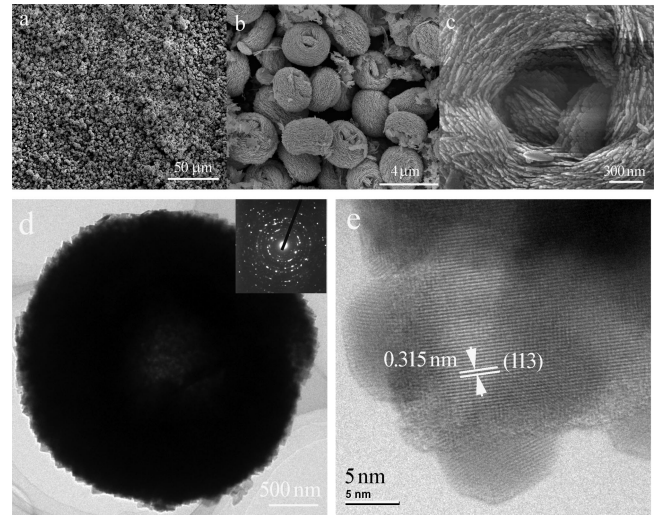

Figure 2. (a) Panoramic FE-SEM image of the products, (b) magnified FE-SEM image, (c) amplified FE-SEM image of an individual hierarchical microsphere, (d) TEM image of an individual microsphere and inserted SAED pattern, (e) HRTEM image taken from the edge of the microsphere.

3. Results and Discussion

The crystallinity and phase purity of the products were examined by XRD measurement. Figure 1 shows a typical XRD pattern of the as-synthesized products. All of reflections can be indexed to pure orthorhombic-phase Bi_2WO_6 [space group *B2cb*], which is in good agreement with the reported data (JCPDS No. 73−1126). After refinement, the crystal lattice parameters of Bi_2WO_6 were calculated: $a = 0.5456$ nm, $b = 1.6445$ nm, and $c = 0.5444$ nm. Widened diffraction peaks show that the size of the crystalline grain is small. According to the Scherrer equation, the crystalline size is ca. 35 nm. Moreover, as can be seen from the XRD pattern, the products indicate high crystallinity. This is beneficial to photocatalysts because high crystallinity generally means fewer traps and stronger photocatalytic activity.[29] The EDX spectrum was further used to determine the chemical composition of as-synthesized products (see Supporting Information Figure S1). The results show that

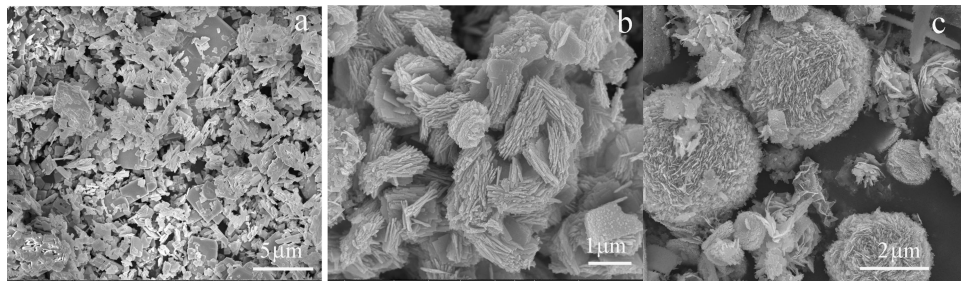

Figure 3. FE-SEM images of the products synthesized: (a) in the absence of citrate, (b) in the absence of $NaHCO_3$, (c) by replacing $NaHCO_3$ with NaOH.

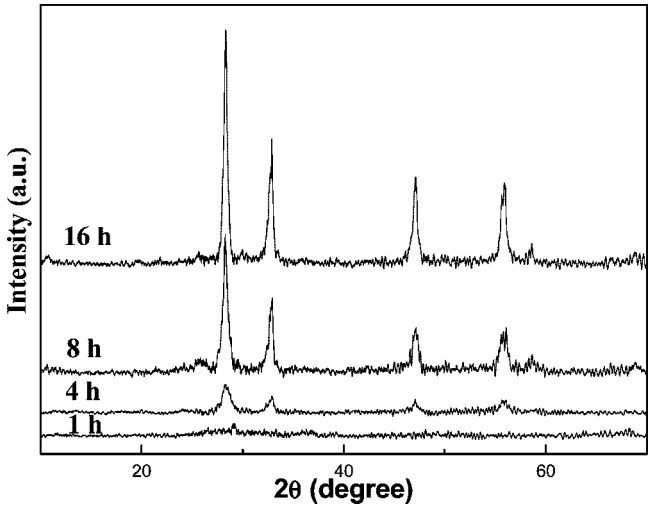

Figure 4. XRD patterns of the samples hydrothermally synthesized at 1, 4, 8, and 16 h, respectively.

the product chiefly consists of W, Bi, O, and C. The ratio of Bi to W and O is 2:0.94:7.17. The ratio of Bi to W is close to stoichiometric proportion of Bi_2WO_6. The superfluous O and the presence of C revealed that the products possibly contained a spot of organic substance.

Figure 2a describes the typical panoramic FE-SEM image of as-synthesized Bi_2WO_6. As can be seen from a low-magnification SEM image (Figure 2a), the sample consists of a large quantity of microspheres. A magnified SEM image (Figure 2b) shows that these microspheres have a 2 μm average diameter and an umbilicate cavity on every microsphere. The surfaces of these microspheres are coarse and have many microstructures on them. An amplified SEM image of an individual microsphere indicates that the microsphere consists of many square nanoplates. Clearly, as-synthesized Bi_2WO_6 microspheres hold three levels of structure. The primary structure is the layered crystal structure of Bi_2WO_6. The secondary structure is the nanosheet assembled from square nanoplates. The tertiary structure is the self-assembled spherical structure from as-formed nanosheets. Figure 2d presents the TEM image of an individual microsphere. The light color in the central section indicates that the Bi_2WO_6 microsphere is hollow in the middle (Figure 2c), which is in accordance with the SEM images. An inserted SAED pattern recorded on the microsphere shows its polycrystalline structure. Figure 2e is the HRTEM image taken from the edge of the microsphere. As can be seen from the HRTEM image, the microsphere consists of several layers of nanosheets. On the top layer, the spacing of the adjacent lattice planes is 0.315 nm, which is consistent with the interplanar spacing of (113) planes of orthorhombic Bi_2WO_6, respectively. This result also displays the single crystal structure of the nanoplates.

With a hydroxyl and three carboxylic groups, citrate is a well-known complexing agent and can form strong complexes with metal ions through a coordination interaction.[41] It can also adsorb strongly on metal[42] and mineral surfaces,[43] significantly alter their surface properties and [44,45] mineral growth behavior,[46] and control the microstructures of large arrays of oriented nanomaterials as well.[47] In our reaction system, citrate plays multifold roles in the formation process of Bi_2WO_6 hierarchical microspheres. It was first used as a complexing agent to control the nucleation and growth rate of Bi_2WO_6. After Bi^{3+} ions with citrate groups formed complexes, the free Bi^{3+} ion concentration would decrease in solution. With an increase in reaction temperature and time under hydrothermal conditions, the chelation of the Bi^{3+}-citrate complex would be weakened and Bi^{3+} would be released gradually. Therefore, the nucleation and growth of Bi_2WO_6 will go through a longer process, which is helpful to form uniform crystals. The released free citrate anions will absorb on the surfaces of firstborn nanoplates again and direct their self-assembly. It is generally believed that the surfaces of nanobuilding blocks stabilized by organic coating tend to oriented aggregation/attachment, and weakly protected nanoparticles often undergo entropy-driven random aggregation.[48] The control experiment shows that the products are irregular and dispersed nanoplates in the absence of citrate (Figure 3a). The FT-IR spectrum of as-synthesized Bi_2WO_6 microspheres indicates that there are characteristic peaks of citrate in the products (see Supporting Information Figure S2). Experimental results confirm the roles of citrate as complexing agent and directing agent for self-assembly of nanoplates.

In our reaction system, $NaHCO_3$ is necessary for formation of the well-defined Bi_2WO_6 microspheres. It could adjust the pH value of the reaction solution as a buffer. We observed that the pH value of the solution after reaction in the absence of $NaHCO_3$ was decreased. However, in the presence of 2 mmol of $NaHCO_3$, the pH value of the solution after reaction are almost unchanged. On the basis of our experiment results and observations, relevant chemical reactions can be proposed as follows:

$$Bi(NO_3)_3 + H_2O \leftrightarrow 2HNO_3 + BiONO_3 \quad \text{(a)}$$

$$BiONO_3 + \text{citrate}^{3-} + H_2O \leftrightarrow \text{Bi-citrate (complex)} + NO_3^- + 2OH^- \quad \text{(b)}$$

$$\text{Bi-citrate (complex)} \leftrightarrow Bi^{3+} + \text{citrate}^{3-} \quad \text{(c)}$$

$$2Bi^{3+} + WO_4^{2-} + 2H_2O \rightarrow Bi_2WO_6 + 4H^+ \quad \text{(d)}$$

$$H^+ + HCO_3^- \leftrightarrow H_2CO_3 \leftrightarrow H_2O + CO_2 \quad \text{(e)}$$

When $Bi(NO_3)_3 \cdot 5H_2O$ was added into water, it gradually reacted with water to form slightly soluble $BiONO_3$, as shown

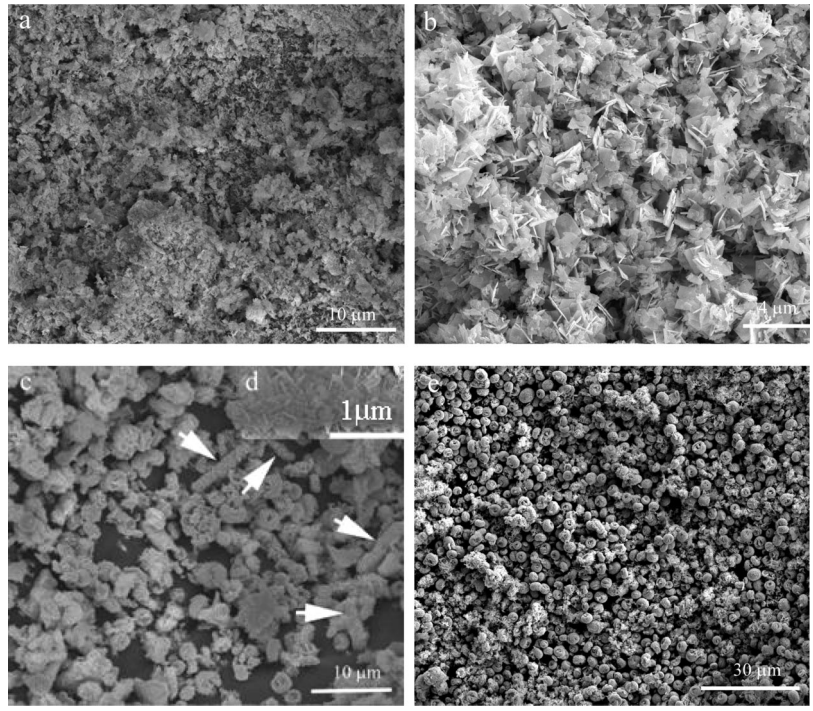

Figure 5. FE-SEM images of the samples hydrothermally synthesized at 200 °C for (a) 1 h, (b) 4 h, (c) 8 h; the inset d is local magnification of a single microrods; (e) 16 h.

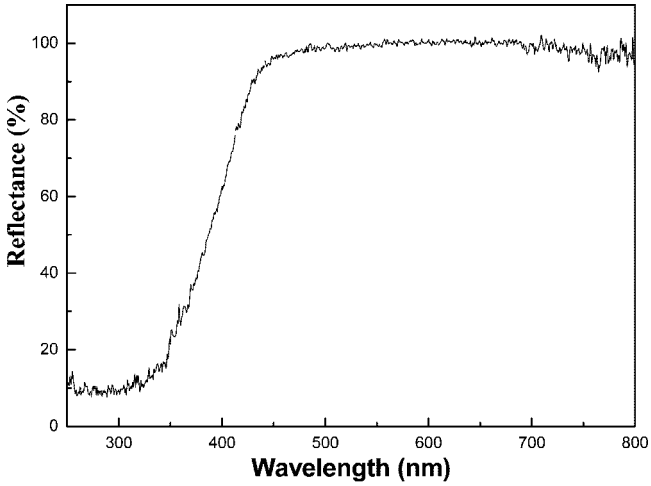

Figure 6. UV−vis diffuse reflectance spectra of the as-synthesized Bi_2WO_6 hierarchical microspheres.

in formula (a). Then, it was transformed into a bicitrate complex as a result of the strong coordination action of Bi^{3+} with citric anions, as shown in formula (b). Under hydrothermal conditions, as the temperature increased, the complex would gradually decompose and slowly release Bi^{3+}, followed by the reaction with WO_4^{2-}, as shown in formulas (c) and (d). Because the solution is acidic, the addition of $NaHCO_3$ will form a buffer system, as shown in formula (e). From the above equations, it can be known that the concentration of H^+ ions will play a rate-determining role in controlling the Bi_2WO_6 concentration within the bulk solution to mediate the nucleation and growth of Bi_2WO_6. Steady pH values are also favorable to assembly of nanoplates into a well-defined morphology. The contrast experiment showed that the products were irregular aggregations of nanoplates in the absence of $NaHCO_3$ (Figure 3b). When $NaHCO_3$ was replaced by NaOH, keeping other conditions unchanged, microspheres built by irregular nanoflakes and dispersed nanoflakes were obtained (Figure 3c). Hence, we believe that $NaHCO_3$ plays an important role in the formation process of Bi_2WO_6 microspheres by adjusting pH values of the reaction solution and establishing a buffer system by the equilibrium of formation and dissociation of carbonic acid.

In order to understand the formation process of Bi_2WO_6 hierarchical microspheres, XRD analysis and SEM observation at the different reaction time periods were carried out. Figure 4 shows XRD patterns of the samples hydrothermally synthesized for 1, 4, 8, and 16 h, respectively. As can be see from these patterns, most of the products are amorphous precursors at the initial 1 h. With the reaction time extended to 4 h, the precursors were transformed into crystalline Bi_2WO_6. As the reaction time was further prolonged, the crystallinity of the products was improved. In order to intuitively understand the morphological evolution process of Bi_2WO_6 microspheres, SEM images were observed at the different time periods. Figure 5a,b,c,e describes SEM images of the products hydrothermally synthesized for 1, 4, 8, and 16 h, respectively. As can be seen from Figure 5a, the products are irregular particles within the initial 1 h. As the reaction time extended to 4 h, these particles were transformed into nanoplates. After 8 h of growth, the products became microspheres and microrods (as the arrowheads show in Figure 5c). A magnified SEM image shows that microrods were also formed by nanoplates (see the inset d). After aging for a longer period up to 16 h, as-obtained products became more regular microspheres and short microrods built from nanoplates disappeared. This phenomenon shows that microrods built from nanoplates took place during the dissolution−recrystallization process, which is often observed in hydrothermal synthesis of nanomaterials.[49] On the basis of the above XRD analysis and SEM observation, the formation mechanism of Bi_2WO_6 hierarchical microspheres was deduced as follows. First, Bi^{3+} and WO_4^{2-} ions slowly formed crystal nuclei from the coordination action of citrate groups. Due to intrinsic anisotropic growth habit of Bi_2WO_6, these first-born crystal nuclei developed into nanoplates under hydrothermal conditions.[29] The citrate adsorbed on the surface of Bi_2WO_6 would direct the self-assembly of

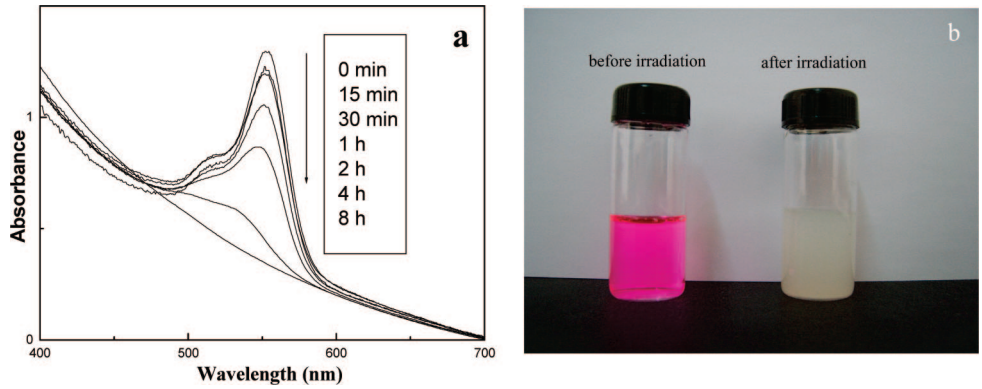

Figure 7. (a) The temporal evolution of the absorption spectrum of the RhB solution (10^{-5} mol/L) in the presence of 100 mg of Bi_2WO_6 under Xe lamp light irradiation. (b) Digital photo of the sample before and after 8 h radiation.

nanoplates by molecular interaction into microspheres and microrods with certain crystallographic orientation. Because sphericity has minimal surface energy, driven by the minimization of the total energy of the system, the microrods built from nanoplates would be dissolved and recrystallized into microspheres assembled by nanoplates under a longer hydrothermal growth process. On the whole, the formation of Bi_2WO_6 hierarchical microspheres went through a nucleation−anisotropic growth−self-assembly−dissolution−reassembly process.

The energy band structure feature of a semiconductor is considered the key factor in determining its photocatalytic activity.[50] Figure 6 represents the UV−vis diffuse reflectance spectra of the as-synthesized Bi_2WO_6 hierarchical microspheres. The absorption edge of the sample extended from the UV light region to ca. 460 nm, which implies the possibility of high photocatalytic activity of this kind of material under Xe lamp light irradiation.

Photocatalytic behavior is closely related to the particle size and surface area. The Brunauer−Emmett−Teller (BET) surface area of the Bi_2WO_6 hierarchical microspheres was calculated using N_2 adsorption data. The BET surface area of the sample was ca. 24.1 m^2/g, which was 35 times higher than that of the reference SSR-Bi_2WO_6 (ca. 0.64 m^2/g).[28] These results indicated that Bi_2WO_6 hierarchical microspheres fabricated from relatively small nanoplates held larger specific surface areas.

In order to evaluate the photocatalytic activities of as-synthesized Bi_2WO_6 hierarchical microspheres, the degradation ability of RhB dye in water under 150 W Xe lamp irradiation was studied. Figure 7a displays the temporal evolution of the spectra during the photodegradation of RhB. RhB has strong absorption at 553 nm. As the exposure time was extended, the position of the absorption peak was shifted to shorter wavelengths and the strength of the peak was reduced. Under Xe lamp illumination, RhB was de-ethylated in a stepwise manner and followed a destruction of the conjugated structure, which had previously been reported in the literature.[51] After 8 h, the absorption peak completely disappeared and the intense pink color of the starting RhB solution faded. Figure 7b shows a digital photo of the sample before and after irradiation for 8 h, indicating the good photocatalytic activity of the as-synthesized Bi_2WO_6 hierarchical microspheres.

The wetting behavior of solid surfaces by a liquid is a very important aspect of surface chemistry, which may have a variety of practical applications.[52−55] Like surfaces with superhydrophobic properties, surfaces that possess superhydrophilicity have also aroused great interest because of their importance for practical applications. For example, superhydrophilicity could improve comfort, perspiration efficiency, and permeability in textile applications. Supporting Information Figure S3 shows the shapes of a water droplet on the original Si wafer and Bi_2WO_6 films fabricated by hierarchical microspheres on the surface of Si wafer, respectively. The contact angle (CA) of water on Bi_2WO_6 films is lower than 5°, which indicates the presence of a superhydrophilic state. It is believed that both surface morphology (e.g., surface roughness) and surface chemical composition strongly affect the surface wettability of the solid materials. Superhydrophilic behavior of the present films can be primarily attributed to the capillary effect.[56] For a hydrophilic solid substrate Si wafer, the hydrophilicitiy will be enhanced by the surface roughness from hierarchical structures of Bi_2WO_6.

4. Conclusions

In conclusion, self-assembled Bi_2WO_6 hierarchical umbilicate microspheres have been successfully synthesized by a designed hydrothermal route. In the formation process of Bi_2WO_6 hierarchical microspheres, citrate played multifold roles. It could be used as a complexing agent to control the nucleation and growth rate of Bi_2WO_6. Additionally, it could selectively absorb on the crystal faces of Bi_2WO_6 nanoplates and direct nanoplate orientation and self-assembly. $NaHCO_3$ could adjust the pH values of the solution and establish a buffer system, which was beneficial to the formation of well-defined Bi_2WO_6 microspheres by the self-assembly mode. XRD analysis and SEM observation of the products showed that the formation process of Bi_2WO_6 hierarchical microspheres mainly went through a nucleation−anisotropic growth−self-assembly−dissolution−reassembly process. Under Xe lamp light irradiation, as-synthesized Bi_2WO_6 microspheres could effectively degrade RhB, which is ascribed to their energy band structures and higher BET surface area. As-prepared films from Bi_2WO_6 microspheres possessing superhydrophilicity could be primarily attributed to the capillary effect related to hierarchical micro/nanocomposite structures. The present method may open up the opportunity to design and synthesize other novel hierarchical materials with special properties.

Acknowledgment. The authors appreciate partial financial support from National Natural Science Foundation of China (Grant Nos. 50772076) and Xinmiao talent project of Zhejiang Province (2007R40G2250033).

Supporting Information Available: EDX spectrum of the as-synthesized products at 200 °C for 18 h (Figure S1), FTIR spectrum of the as-synthesized products at 200 °C for 18 h

(Figure S2), and shapes of the water droplets on (a) the original Si wafer and (b) the Bi_2WO_6 films obtained by drop-casting an ethanolic suspension of as-synthesized hierarchical microspheres onto the Si wafer (Figure S3). This material is available free of charge via the Internet at http://pubs.acs.org.

References and Notes

(1) Wang, X.; Zhuang, J.; Peng, Q.; Li, Y. D. *Nature* **2005**, *437*, 121.
(2) Xia, Y. N.; Yang, P. D. *Adv. Mater.* **2003**, *15*, 351.
(3) Pan, Z. W.; Dai, Z. R.; Wang, Z. L. *Science* **2001**, *291*, 1947.
(4) Zhang, Y. W.; Sun, X.; Si, R.; You, L. P.; Yan, C. H. *J. Am. Chem. Soc.* **2005**, *127*, 3260.
(5) Li, M.; Schnablegger, H.; Mann, S. *Nature* **1999**, *402*, 393.
(6) Park, S.; Lim, J. H.; Chung, S. W.; Mirkin, C. A. *Science* **2004**, *303*, 348.
(7) Liu, B.; Zeng, H. C. *J. Am. Chem. Soc.* **2004**, *126*, 8124.
(8) Tian, Z. R. R.; Voigt, J. A.; Liu, J.; Mckenzie, B.; Mcdermott, M. J. *J. Am. Chem. Soc.* **2006**, *128*, 10960.
(9) Cöfen, H.; Mann, S. *Angew. Chem., Int. Ed.* **2003**, *42*, 2350.
(10) Shi, H. T.; Qi, L. M.; Ma, J. M.; Cheng, H. M. *J. Am. Chem. Soc.* **2003**, *125*, 3450.
(11) Zhang, Z. P.; Sun, H. P.; Shao, X. Q.; Li, D. F.; Yu, H. D.; Han, M. Y. *Adv. Mater.* **2005**, *17*, 42.
(12) Liu, B.; Zeng, H. C. *J. Am. Chem. Soc.* **2004**, *126*, 16744.
(13) Caruso, R. A.; Schattka, J. H.; Greiner, A. *Adv. Mater.* **2001**, *13*, 1577.
(14) Dinsmore, A. D.; Hsu, M. F.; Nikolaides, M. G.; Marquez, M.; Bausch, A. R.; Weitz, D. A. *Science* **2002**, *298*, 1006.
(15) Zhu, J. J.; Xu, S.; Wang, H.; Zhu, J. M.; Chen, H. Y. *Adv. Mater.* **2003**, *15*, 156.
(16) Zhang, T. R.; Dong, W. J.; Keeter-Brewer, M.; Konar, S.; Njabon, R. N.; Tian, Z. R. *J. Am. Chem. Soc.* **2006**, *128*, 10960.
(17) Murray, C. B.; Kagan, C. R.; Bawendi, M. G. *Science* **1995**, *270*, 1335.
(18) Manna, L.; Scher, E. C.; Alivisatos, A. P. *J. Am. Chem. Soc.* **2000**, *122*, 12700.
(19) Aurivillius, B. *Ark. Kemi* **1952**, *5*, 39.
(20) McDowell, N. A.; Knight, K. S.; Lightfoot, P. *Chem. Eur. J.* **2006**, *12*, 1493.
(21) Stefanovich, S. Y.; Nenetsev, Y. N. *Phys. Status Solidi A* **1973**, *20*, 49.
(22) Ismailzade, I. G.; Mirishli, F. A. *Kristallografiya* **1970**, *14*, 738.
(23) Yanovskii, V. K.; Voronkova, V. I.; Alexandrovskii, A. L.; D'yakov, V. A. *Dokl. Akad. Nauk SSSR* **1975**, *222*, 94.
(24) Utkin, V. I.; Roginsksya, Y. E.; Voronkova, V. I.; Yanovskii, V. K.; Galyamov, B. S.; Venetsev, Y. N. *Phys. Status Solidi A* **1980**, *59*, 75.
(25) Herwood, P. *Ind. Chem.* **1963**, *39*, 242.
(26) Bordun, O. M. *Inorg. Mater.* **1998**, *34*, 12.
(27) Kudo, A.; Hijii, S. *Chem. Lett.* **1999**, *10*, 1103.
(28) Tang, J. W.; Zou, Z. G.; Ye, J. H. *Catal. Lett.* **2004**, *92*, 53.
(29) Zhang, C.; Zhu, Y. F. *Chem. Mater.* **2005**, *17*, 3537.
(30) Fu, H. B.; Pan, C. S.; Yao, W. Q.; Zhu, Y. F. *J. Phys. Chem. B* **2005**, *109*, 22432.
(31) Fu, H. B.; Zhang, L. W.; Yao, W. Q.; Zhu, Y. F. *App. Catal. B* **2006**, *66*, 100.
(32) Shang, M.; Wang, W. Z.; Sun, S. M.; Zhou, L.; Zhang, L. *J. Phys. Chem. C* **2008**, *112*, 10407.
(33) Zhang, L. S.; Wang, W. Z.; Zhou, L.; Xu, H. L. *Small* **2007**, *3*, 1618.
(34) Li, Y. Y.; Liu, J. P.; Huang, X. T.; Li, G. Y. *Cryst. Growth Des.* **2007**, *7*, 135.
(35) Wu, J.; Duan, F.; Zheng, Y.; Xie, Y. *J. Phys. Chem. C* **2007**, *111*, 12866.
(36) Amano, F.; Nogami, K.; Abe, R.; Ohtani, B. *J. Phys. Chem. C* **2008**, *112*, 9320.
(37) Feng, X.; Feng, L.; Jin, M.; Zhai, J.; Jiang, L.; Zhu, D. B. *J. Am. Chem. Soc.* **2004**, *126*, 62.
(38) Feng, X.; Zhai, J.; Jiang, L. *Angew. Chem., Int. Ed.* **2005**, *44*, 5115.
(39) Sun, T. L.; Feng, L.; Gao, X. F.; Jiang, L. *Acc. Chem. Res.* **2005**, *38*, 644.
(40) Wang, D. A.; Guo, Z. G.; Chen, Y. M.; Hao, J. C.; Liu, W. M. *Inorg. Chem.* **2007**, *46*, 7707.
(41) Huignard, A.; Buissette, V.; Laurent, G.; Gacoin, T.; Boilot, J. P. *Chem. Mater.* **2002**, *14*, 2264.
(42) Jolivet, J. P.; Gzara, M.; Mazieres, J.; Lefebvre, *J. Colloid Interface Sci.* **1985**, *107*, 429.
(43) López-Macipe, A.; Gómez-Morales, J.; Rodríguez-Clemente, R. *J. Colloid Interface Sci.* **1998**, *200*, 114.
(44) Hidber, P. C.; Graule, T. J.; Gauckler, L. J. *J. Am. Ceram. Soc.* **1996**, *79*, 1857.
(45) Biggs, S.; Scales, P. J.; Leong, Y. K.; Healy, T. W. *J. Chem. Soc. Faraday Trans.* **1995**, *91*, 2921.
(46) Liu, C.; Huang, P. M. *Soil. Sci. Soc. Am. J.* **1999**, *63*, 65.
(47) Tian, Z. R. R.; Voigt, J. A.; Liu, J.; Mckenzie, B.; Mcdermott, M. J.; Rodriguez, M. A.; Konishi, H.; Xu, H. F. *Nat. Mater.* **2003**, *2*, 821.
(48) Zhang, Z. P.; Sun, H. P.; Shao, X. Q.; Li, D. F.; Yu, H. D.; Han, M. Y. *Adv. Mater.* **2005**, *17*, 42.
(49) Xi, G. C.; Xiong, K.; Zhao, Q. B.; Zhang, R.; Zhang, H. B.; Qian, Y. T. *Cryst. Growth Des.* **2006**, *6*, 577.
(50) Tang, J. W.; Zou, Z. G.; Ye, J. H. *Angew. Chem., Int. Ed.* **2004**, *43*, 4463.
(51) Zhao, W.; Chen, C. C.; Li, X. Z.; Zhao, J. C. *J. Phys. Chem. B* **2002**, *106*, 5022.
(52) Wenzel, R. N. *Ind. Eng. Chem.* **1936**, *28*, 988.
(53) Blossey, R. *Nat. Mater.* **2003**, *2*, 301.
(54) Liu, Y.; Mu, L.; Liu, B. H.; Kong, J. L. *Chem. Eur. J.* **2005**, *11*, 2622.
(55) Parkin, I. P.; Palgrave, R. G. *J. Mater. Chem.* **2005**, *15*, 1689.
(56) Feng, X. J.; Jiang, L. *Adv. Mater.* **2006**, *18*, 3063.

JP810726D